AIP | Journal of Applied Physics

Structural, electronic, and optical aspects of Cr doping of the Bi4Ge3O12: An ab initio study

A. F. Lima and M. V. Lalic

Citation: J. Appl. Phys. 108, 083713 (2010); doi: 10.1063/1.3500452
View online: http://dx.doi.org/10.1063/1.3500452
View Table of Contents: http://jap.aip.org/resource/1/JAPIAU/v108/i8
Published by the AIP Publishing LLC.

Structural, electronic, and optical aspects of Cr doping of the $Bi_4Ge_3O_{12}$: An *ab initio* study

A. F. Lima and M. V. Lalic[a)]
Departamento de Física, Universidade Federal de Sergipe, P.O. Box 353, 49100-000 São Cristóvão/SE, Brazil

(Received 3 July 2010; accepted 7 September 2010; published online 22 October 2010)

Ab initio calculations based on density functional theory have been employed to study energetic, structural, electronic, and optical properties of Cr doped $Bi_4Ge_3O_{12}$ (BGO). Two possible accommodations of Cr impurity have been taken into account: at the Ge (Cr^{4+}) and the Bi (Cr^{3+}) substitution site. For each accommodation the local structure around the Cr has been determined, and in the Cr^{3+} case the Cr off-site displacement was analyzed. The Cr *d*-states are positioned at the bottom of the conduction band and within the gap in form of two deeplike (Cr^{4+}) and shallowlike (Cr^{3+}) bands, exhibiting magnetic moments of +1.58 μ_B and −2.44 μ_B, respectively. The Cr dominated part of absorption spectrum is calculated and analyzed in terms of Cr band arrangement. Comparison with the experimental BGO:Cr absorption spectrum suggests that it consists of both Cr^{3+} and Cr^{4+} contributions, indicating the Cr simultaneous presence at both substitution sites.
 [doi:10.1063/1.3500452]

I. INTRODUCTION

The bismuth orthogermanate $Bi_4Ge_3O_{12}$ (BGO) has been extensively studied due to its excellent scintillation properties suitable for technological applications. In its pure form it is utilized as high-efficient scintillator in scientific research[1] and nuclear medicine diagnostic systems.[2] Furthermore, it exhibits useful electro-optics properties such as a possibility to record holographic gratings at shorter ultraviolet wavelengths at room temperature.[3]

Analysis of doped and undoped BGO samples shows that nominally undoped crystals contain few parts per million of iron and chromium atoms.[4] These impurities play important role providing extra levels within the band gap and changing the optical properties of pure compound.[5] Particularly, the Cr impurity is responsible for self-absorption of light generated during the scintillation process, which substantially decrease the light output and the radiation resistance of the BGO crystal.[6,7] On the other hand, the Cr presence significantly enhances photorefractive response of the BGO (Ref. 8) and improves its potential to be used as a tunable near infrared solid state laser host.[9]

Several experimental studies have been performed on the Cr doped BGO system (BGO:Cr) so far, being mainly focused on its optical properties and possible Cr accommodation within the lattice. They, however, offer controversial interpretations of the observed optical absorption spectra. On the basis of optical spectroscopy investigations, Chernei *et al.*[10] and de Mello *et al.*[7] assume that all absorption bands originate from transitions between levels caused by presence of the Cr^{4+} ion at the tetrahedral Ge^{4+} site, while the Yingpeng *et al.*[11] attribute origin of these bands to the presence of both the Cr^{3+} and Cr^{4+} ions at the Ge^{4+} positions. Neither of these studies considers a possibility of Cr occupation of the octahedral Bi^{3+} site, as indicated by electron paramagnetic resonance (EPR) studies of Bravo and Lopez.[9] The latter shows that Cr impurity can appear in both 4+ and 3+ valence states, substituting the Ge^{4+} and Bi^{3+} sites, respectively, without need of any charge compensation. The concentration of the Cr^{3+} ions is, however, estimated to be about 50 times lesser.[9] Theoretical study of Wu and Dong,[12] based on application of perturbation formulas on EPR parameters, analyses the Cr situated at the Bi site and indicates the Cr off-site displacement toward the center of O's octahedron around it.

The present study has two main objectives: (1) to analyze theoretically the structural, energetic, electronic, and especially optical characteristics of Cr doped BGO, and (2) to confront obtained results with previously determined experimental and theoretical findings, mentioned above. In order to comprise these goals, we employed the first-principles density-functional theory (DFT) based calculations and treated doped BGO crystal with substitutional Cr impurities situated either at the Ge^{4+} or at the Bi^{3+} site. The calculated properties were compared with ones recently determined for the pure BGO crystal,[13,14] which enabled us to extract the effects caused by Cr presence. Results of atomic relaxations around the impurity showed that the Cr^{3+} suffers off-site displacement away from the center of O's octahedron around it, not supporting the Wu and Dong prediction.[12] Analysis of optical absorption spectrum and its comparison with available experimental data indicates that it is composed of contributions from both the Cr^{4+} and Cr^{3+} ions residing simultaneously at the Ge^{4+} and the Bi^{3+} positions, respectively.

II. CRYSTAL STRUCTURE AND CALCULATION DETAILS

The BGO crystallizes in cubic symmetry, space group *I*43*d*. Its primitive unit cell contains two formula units (38 atoms), without having a center of inversion. The building blocks of crystal structure are $(BiO_6)^{9-}$ octahedrons and $(GeO_4)^{4-}$ tetrahedrons, linked in irregular manner, as shown

[a)]Electronic mail:mlalic@ufs.br.

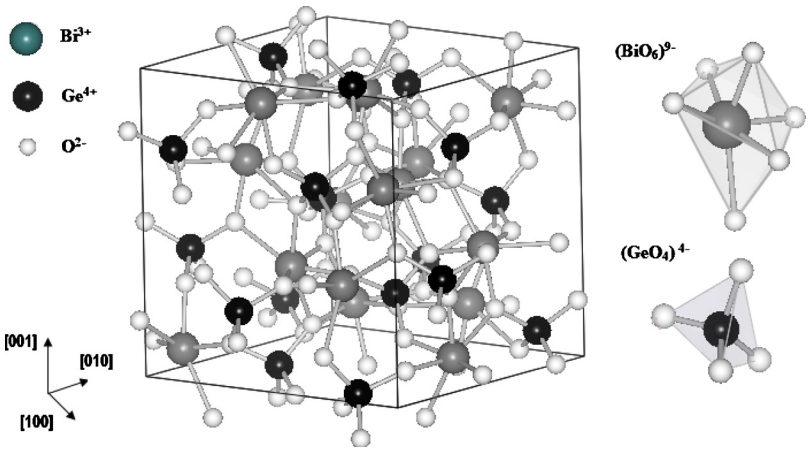

FIG. 1. (Color online) Crystal structure of the pure $Bi_4Ge_3O_{12}$. Each Bi^{3+} ion is surrounded by six O's ions forming a $(BiO_6)^{9-}$ distorted octahedron, while each Ge^{4+} ion is coordinated by four O's ions arranged in a $(GeO_4)^{4-}$ tetrahedron.

in the Fig. 1. Each Bi^{3+} ion is surrounded by six oxygen's arranged in vertices of strongly distorted octahedron: three of them (O_1) are situated nearer to the Bi than the other three (O_2). The Bi senses the C_3 point symmetry with trigonal (C_3) axis pointing along a [111] direction of the cubic cell. The Ge^{4+} ion is coordinated by four oxygen's arranged in the vertices of tetrahedron very slightly compressed along its [100] fourfold symmetry axis. If the tetrahedron were perfect, the Ge would sense the S_4 point symmetry.

In present work we study two imperfect BGO systems: the BGO with Cr which substitutes the Bi (BGO:Cr→Bi case) and the BGO with Cr which substitutes the Ge (BGO:Cr→Ge case). Doped systems were simulated using the primitive unit cell of the pure BGO (Ref. 14) from which the central Bi (or Ge) atom has been removed and replaced by the Cr atom. The crystal is then generated by infinite repetition of this unit cell. Therefore, we have actually simulated doped BGO crystal with Cr concentration of 1/38 (2.6%). Due to extensive unit cell of the BGO, the Cr–Cr distance is large enough to prevent significant interaction between them. All atomic positions around impurity were allowed to relax by total energy minimization, while the unit cell parameter was kept fixed, a=10.594 Å.[14] Structural relaxation has been carried out until the force sensed by any atom in unit cell reached the value lesser than 2 mRy/a.u.

The self-consistent band-structure calculations were performed by DFT (Ref. 15) based, full potential linear augmented plane wave (FP-LAPW) method[16] as embodied in WIEN2K computer code.[17] In this method, the electronic wave functions, charge density, and crystal potential are expanded in spherical harmonics inside nonoverlapping spheres centered at each nuclear position (atomic spheres), and in plane waves in the rest of the space (interstitial region). The choice for the atomic sphere radii R_{MT} (in atomic units) was 2.3 for the Bi, 1.8 for the Ge, 1.45 for the O, and 1.8 for the Cr atom. Inside atomic spheres the partial waves were expanded up to $l_{max}=10$, while the number of plane waves in the interstitial was limited by the cut-off at $K_{max}=7.0/R_{MT}$. The augmented plane waves were utilized as a basis set. The charge density was Fourier expanded up to $G_{max}=14$. For k-space integration a mesh of 12 k-points in the irreducible part of the Brillouin zone (IBZ) was used. Exchange and correlation effects were treated by generalized-gradient approximation (GGA).[18] The Bi 5*d*, 6*s*, 6*p*, the O 2*s*, 2*p*, the Ge 3*d*, 4*s*, 4*p*, and the Cr 3*s*, 3*p*, 3*d*, and 4*s* electronic states were considered as valence ones, and treated within the scalar-relativistic approach, whereas the core states were relaxed in fully relativistic manner. Three types of band-structure calculations were performed, in following sequence: (1) nonmagnetic, (2) spin-polarized, and (3) spin-polarized with the spin-orbit coupling accounted for heavy Bi atoms. This approach permitted us to estimate the importance of spin polarization and spin-orbit interaction on calculated properties.

Optical response is determined by calculating the complex dielectric tensor ε. Imaginary part of this tensor is directly proportional to the intensity of the optical absorption of the material. It can be computed from knowledge of the electronic band structure. In the limit of linear optics, neglecting electron polarization effects and within the frame of random phase approximation, the expression for the imaginary part of ε is the following:[19]

$$\mathrm{Im}\,\varepsilon_{\alpha\beta}(\omega)=\frac{4\pi^2e^2}{m^2\omega^2}\sum_{i,f}\int_{BZ}\frac{2dk}{(2\pi)^3}|\langle\varphi_{fk}|P_\beta|\varphi_{ik}\rangle| \times|\langle\varphi_{fk}|P_\alpha|\varphi_{ik}\rangle|\cdot\delta(E_f(k)-E_i(k)-\hbar\omega), \quad (1)$$

for a vertical transition from a filled initial state $|\varphi_{ik}\rangle$ of energy $E_i(k)$ to an empty final state $|\varphi_{fk}\rangle$ of energy $E_f(k)$ with the same wave vector k. ω is the frequency of the incident radiation, m the electron mass, P the momentum operator, and α and β stand for the projections x, y, and z of incident wave polarization.

We computed the Im(ε) up to incident radiation energy of $\hbar\omega=40$ eV, with a mesh of 55 (BGO:Cr→Ge case) and 68 k-points (BGO:Cr→Bi case) in the irreducible wedge of the first Brillouin zone. Owing to the cubic symmetry of the BGO, the dielectric tensor is diagonal, with $\varepsilon_{xx}=\varepsilon_{yy}=\varepsilon_{zz}=\varepsilon$. Thus, in this particular case, it is reduced to scalar function $\varepsilon(\omega)$.

III. RESULTS AND DISCUSSION

A. Defect formation energies

In order to estimate energies required for substitution of the Ge (or Bi) atoms for Cr in the BGO structure, we calculated defect formation energies E_d according to the following formula:

TABLE I. Defect formation energies for two different accommodations of the Cr impurity within the BGO crystal lattice, as calculated by the FP-LAPW method.

	Nonmagnetic calculations	Spin-polarized calculations	Spin-polarized+SO calculations
$E_{Cr\rightarrow Bi}$	−1.720	−0.169	−0.392
$E_{Cr\rightarrow Ge}$	−0.658	−0.549	−0.431

$$E_d = [E_{Pure\ BGO} + E_{Free\ Cr}] - [E_{BGO:Cr} + E_{Free\ Bi\ or\ Ge}], \quad (2)$$

where the first bracket represents the sum of the total energies of the pure BGO unit cell (taken from the Ref. 14) and the free Cr atom, while the second represents the total energy of the unit cell of the BGO containing the Cr (either at the Bi or the Ge site) plus the energy of the free Bi or Ge atoms which are removed from unit cell to make room for the impurity. The energies of the pure and the doped BGO crystal were computed on the same precision level and with the same computation parameters (number of k-points, atomic sphere radii, etc.), for each type of calculations performed. The free atoms were computationally treated in the same manner as the BGO crystals. For this purpose it was created an infinite structure consisting of very large cubic unit cells (lattice parameter was 30 atomic units) with the atoms in their centers. Because the atoms are very far from each other, the mutual interaction could be neglected. The free atom energies in (2) were then calculated as the unit cell energies by the spin-polarized FP-LAPW method, using one k-point in the IBZ. This procedure assured the same precision of calculated free-atom and crystal energies, enabling their comparison in (2).

Table I presents the defect formation energies for two possible accommodations of the Cr ion, resulting from three types of band-structure calculations. It should be noticed that the substitutional doping is energetically more favorable when the energy values are smaller. As can be seen, these values strongly depend on precision of the calculations. The most precise one, with the spin-orbit coupling switched on, shows very slight Cr preference to substitute the Ge atom. The energy of the Cr substitution of the Bi atom is, however, only 0.039 eV higher. Both energies are negative, which indicates that Cr impurity can be easily incorporated into the host crystal, and into the both available positions. Table I stresses importance of relativistic treatment of the Bi electronic states, a fact that has been proved in previous *ab initio* studies of pure BGO.[14,20]

B. Local structure around the impurity

Information about local structures around Cr impurities was accessed via computational relaxation of atomic positions in BGO:Cr crystal. This information can be useful for interpretation of optical and EPR spectroscopic data. The local structures which depict the first neighborhood around the Bi and Ge sites within the pure BGO are usually described in terms of two parameters: (1) the metal–oxygen distance R_{M-O}, and (2) the angle β between the R_{M-O} and either the S_4 (Ge) or C_3 (Bi) axis. The same parameters are utilized to describe the Cr surroundings in the BGO:Cr systems as well. Table II shows these parameters as calculated in the present work, together with the parameters previously calculated and experimentally determined for pure BGO.

It is seen from the Table II that the Cr presence at the Ge site causes very small deformation of its surrounding, since both parameters R_{M-O} and β remain very similar to the ones that describe the Ge neighborhood in the pure compound. The process of substitution of Ge by Cr is therefore smooth and accompanied by the decrease in energy (Table I).

When substitutes the Bi atom, however, the Cr produces significant changes on its surrounding. Table II shows large difference between parameters which characterize the Cr neighborhood and the unperturbed Bi neighborhood. Such a different local structure around the Cr arises not just from relaxation of neighboring O's but from movement of the Cr itself. A more detailed analysis based on comparison of atomic positions of the Cr and its six neighboring O's before and after the computational optimization reveals that a dislocation suffered by the Cr ion is about ten times larger than dislocations experienced by the O's. The same analysis shows that Cr dislocates along the [111] direction, which coincides with the trigonal C_3 axis. This leads to the conclusion that the local structure around Cr is dominantly determined by its proper dislocation from ideal host (i.e., Bi) position. Although the Cr entrance to the Bi site produces much

TABLE II. Calculated equilibrium Cr–O bond lengths (in Å) and angles β between them and either the S_4 (Cr→Ge case) or C_3 (Cr→Bi case) axis in the BGO:Cr, compared to the previous theoretical and experimental data for the pure BGO. The labels O_1 and O_2 denote the three nearest and the three second nearest Bi neighbors, respectively. The numbers in parenthesis denote number of oxygens which correspond to the given bond length and the angle.

	Pure BGO		BGO:Cr
	Experiment[a]	Theory[b]	This work
			(Cr→Ge)
Ge–O	1.73 (4) β=58.06°	1.782 (4) β=59.47°	1.774 (4) β=59.88°
			(Cr→Bi)
Bi–O_1	2.149 (3) β=51.38°	2.221 (3) β=50.11°	1.864 (3) β=60.50°
Bi–O_2	2.620 (3) β=104.62°	2.583 (3) β=102.77°	2.575 (3) β=113.51°

[a]Reference 21.
[b]Reference 14.

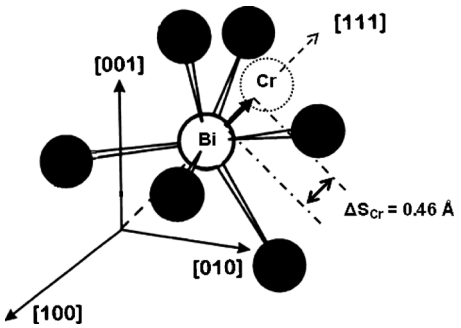

FIG. 2. Off-site displacement of the Cr impurity which substitutes the Bi site in the BGO. The Cr moves along the [111] direction toward the three nearest O's, away from the center of the imaginary octahedron with O's at its vertices.

larger lattice relaxation, this process leads to practically same energy gain as the Cr entrance to the Ge position, as seen from the Table I.

Off-site displacement of Cr from Bi site in the BGO:Cr has already been reported by Wu and Dong[12] who applied perturbation formulas on the EPR parameters for an d^3 ion in trigonally-distorted octahedral environment, and predicted that the Cr should displace along the C_3 axis in the direction toward the center of the octahedron of O's around it. The estimated value of this displacement was 0.17 Å. The authors explained this result by assuming that the Cr^{3+}, having a slightly smaller ionic radius then the Bi^{3+}, feels loose environment at the Bi^{3+} position, which pushes it in the direction toward the center of the oxygen octahedron.

Present DFT calculations confirm the Wu and Dong conclusion about the Cr dislocation along the C_3 axis but disagree with the predicted direction. According to data presented in the Table II, the Cr approaches to its three nearest O neighbors, which is evident if one compares the Bi–O bond lengths for the ideal host position of the Cr (first or second column of the Table II) with the Cr–O bond lengths for the relaxed position of the Cr (third column of the Table II). At the same time, both angles β which correspond to the Cr–O bonds increase, which is consistent with described movement of the Cr. Table II shows that the $Cr-O_1$ and $Cr-O_2$ bond lengths in the BGO:Cr differ more than the corresponding $Bi-O_1$ and $Bi-O_2$ bond lengths in the pure BGO. All these facts lead to the conclusion that the Cr suffered off-site dislocation away from the center of the oxygen octahedron along the C_3 axis (Fig. 2). We calculated this displacement to be 0.46 Å.

The reason for disagreement between our calculations and conclusions of Wu and Dong might be a fact that Wu and Dong[12] extensively used the concept of ionic radius throughout their calculations. This concept works much better for highly ionic compounds, which is not the case of the BGO:Cr. The Cr–O bond in the BGO has significant covalent character due the hybridization of the Cr *s*-state and *d*-state with the nearest O's *p*-states (which is evident from the Fig. 4 presented in Sec. III C). Therefore, assigning any definite value for the size of the Cr^{3+} and the Bi^{3+} ions in the BGO might be questionable. A recent DFT analysis of local structure around the Nd^{3+} which substitutes the Bi site in the BGO showed the same disagreement about direction of the impurity displacement along the C_3 axis: while the Wu and Dong conclude that Nd should move away from the center of O's octahedron,[12] the DFT predicts the opposite.[22]

C. Electronic structure

Figure 3 shows the band structure, total, and partial density of states (TDOS and PDOS, respectively) of the BGO:Cr→Ge system, resulted from the spin-polarized calculation with the spin-orbit interaction taken into account for Bi atoms. The principal difference between the TDOS presented at the Fig. 3(a) and the TDOS of the pure BGO (Ref. 14) consists of a presence of bands which are situated either within the gap or at the lowest-energy part of the conduction

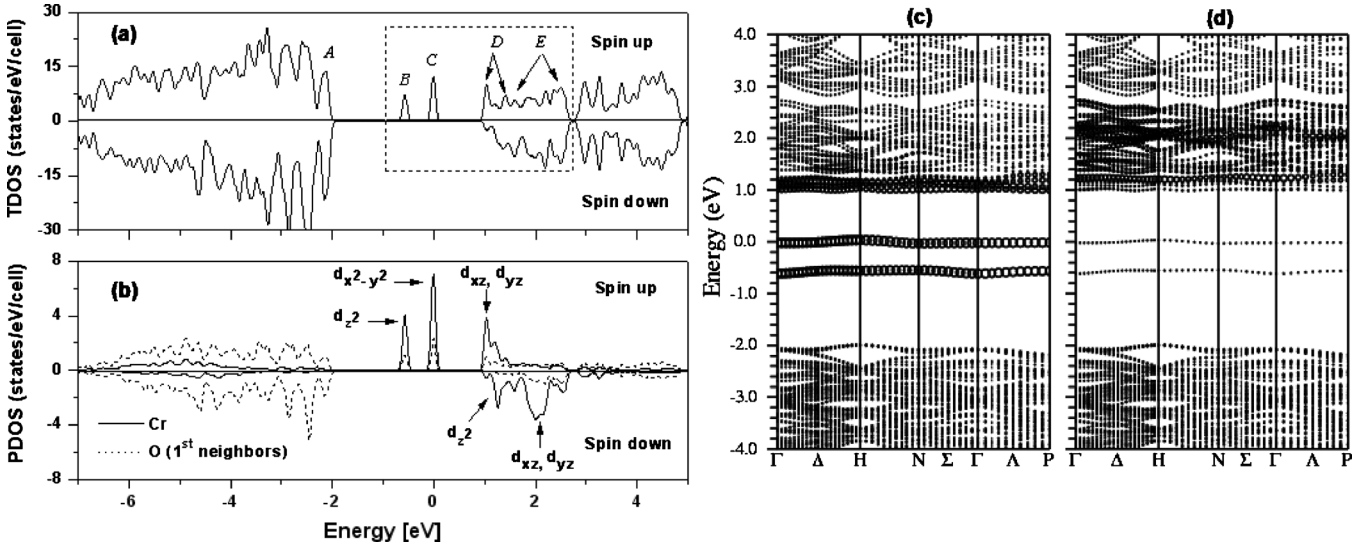

FIG. 3. Calculated electronic structure of the BGO with the Cr at the Ge position. (a) The total spin-polarized electronic density of states, where the Cr contribution is emphasized by the square; letters *A*-*E* denote bands important for analysis of the absorption spectrum. (b): the PDOS showing the Cr and its four neighboring O's states only. (c) and (d) show energy bands along high symmetry directions within the first Brillouin zone. (c) emphasizes the Cr *d* spin up states using larger circles, while the figure (d) does the same with the Cr *d* spin down states.

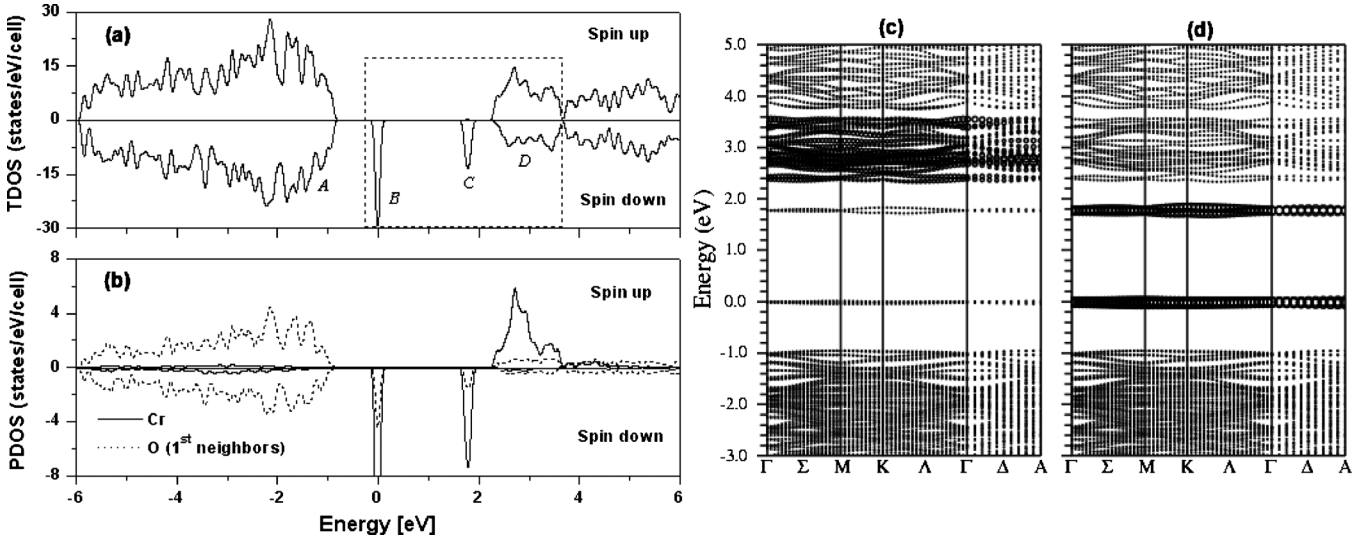

FIG. 4. Calculated electronic structure of the BGO with the Cr at the Bi position. (a) The total spin-polarized electronic density of states, with the Cr contribution (*d*-states) emphasized by the square; letters *A*-*D* denote bands important for analysis of the absorption spectrum. (b) The PDOS showing the Cr and neighboring O's states only. Figures (c) and (d) show energy bands along high symmetry directions within the first Brillouin zone. The figure (c) emphasizes the Cr *d* spin up states using larger circles, while the figure (d) does the same with the Cr *d* spin down states.

band (where mixed with the Bi *p*-states). These bands are emphasized by the square on the Fig. 3(a). All of them have substantially Cr d-character. Two deeplike bands within the gap are occupied, each with one electron, with energy difference between them of about 0.6 eV. This fact demonstrates that the DFT-GGA calculations correctly described the 4+ ionization state of the Cr ($3d^2$ configuration). Energy difference between the highest occupied band (HOB) and the lowest unoccupied band (LUB) is approximately 1.1 eV, which is the lowest excitation energy expected in the BGO:Cr $\rightarrow$Ge system. All Cr *d*-states within the gap are strongly hybridized with the *p*-states of nearest neighbor O's, which is seen from the PDOS shown at the Fig. 3(b). This fact causes the broadening of bands. Deep band of lower energy consists of the Cr (d_{z2}) states, where the z-axis is directed along the S_4 symmetry axis. Deep band of higher energy consists of superposition of the Cr d_{xy} and d_{x2-y2} states, while the band at the conduction band bottom is formed from the Cr (d_{z2}) and d_{yz} spin-up states and the d_z^2 spin-down states. Majority states are the spin-up, and calculated magnetic moment of Cr is +1.58 μ_B. The composition of other bands which originate from the host BGO matrix, unaffected by the Cr presence, is the same as previously reported.[14]

Figure 4 shows the band structure, TDOS and PDOS of the BGO:Cr$\rightarrow$Bi system, as resulted from the spin-polarized calculations with spin-orbit coupling accounted for the Bi atoms. The Cr *d*-states are partially positioned within the BGO gap and partially mixed with the Bi 6*p*-states at the bottom of the conduction band. These states are emphasized by the square at the Fig. 4(a). Two bands within the gap could be characterized as shallowlike ones, as being located near the gap edges. The one with lower energy is fully occupied (HOB), containing three electrons, and another one is empty (LUB). This situation correctly describes the 3+ ionization state of the Cr ($3d^3$ configuration). Contrary to the case of the BGO:Cr$\rightarrow$Ge system, all the Cr *d*-bands have mixed orbital characters which prevents their clear orbital characterization. They are strongly hybridized with the neighboring O's *p*-states, as can be seen from the Fig. 4(b). Energy difference between the *HOB* and *LUB* is around 1.8 eV, significantly higher comparing to the BGO:Cr$\rightarrow$Ge case. Majority states are spin-down, and the magnetic moment of the Cr atom is calculated to be −2.44 μ_B.

D. Optical absorption spectrum

Optical properties of the BGO:Cr compounds were investigated in energy interval from 0 to 3.5 eV in which the pure BGO does not absorb at all and the Cr impurity makes its contribution. Figure 5 presents the calculated optical absorption spectrum of the BGO:Cr$\rightarrow$Ge system, as well as the simplified electron energy diagram which explains it. The figure reveals several prominent structures below absorption edge of the pure BGO which are identified by numbers I–IV. All of them are caused by Cr presence within the BGO matrix and can be interpreted on the basis of the band structure presented at the Fig. 3, using the band nomenclature introduced there. The structure I, centered on 1.1 eV, originates from electronic transitions between *d*-states of the Cr, from the band $C(d_{x^2-y^2})$ to the band D (d_{xy}, d_{xz}). The structure II, centered on about 1.8 eV, is also created by transitions between the Cr *d*-states, from the band B (d_{z^2}) to the band D (d_{xy}, d_{xz}) These transitions are not dipole-forbidden because the BGO unit cell does not possess inversion center. The structure III is formed by electron promotions from the bands *B* and *C* to the band *E*. Since the latter have very little spin-up states at disposal, and the bands *B* and *C* contain exclusively this type of states, the transition intensity is very low. That is why the structure III is much less pronounced and more dispersed comparing to other structures. Finally, the structure IV, positioned between 3.2 and 3.5 eV, is dominantly caused by electron promotions from the band *A* to the band *D*, mostly involving transitions between empty and populated O *p* states. This structure, however, already makes

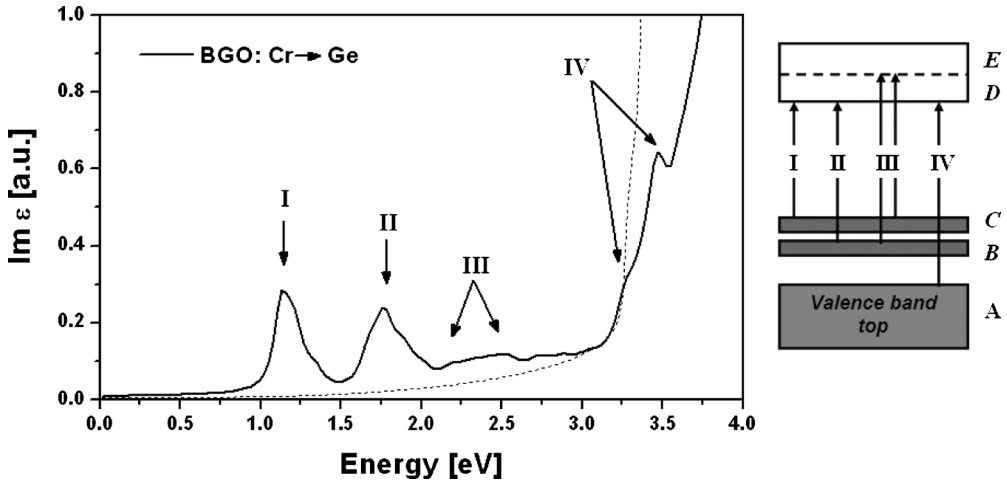

FIG. 5. Left: intensity of optical absorption of the BGO:Cr→Ge (in arbitrary units) as function of incident radiation energy. Dotted curve represents optical absorption of the pure BGO. Right: energy band diagram of the BGO:Cr→Ge constructed on the basis of the band structure shown at the Fig. 3, where the band notation *A*-*E* is defined. The numbers associated with vertical arrows indicate electronic transitions responsible for the corresponding structures in the optical spectrum.

part of continuous conduction band. All described transitions are represented by vertical arrows at the energy diagram on the right part of the Fig. 5.

The calculated absorption spectrum of the BGO:Cr →Bi system is presented on the Fig. 6 (left), together with the energy diagram which helps to interpret it (right). The spectrum is much simpler then the BGO:Cr→Ge spectrum mostly due to specific arrangement of the Cr spin-down and spin-up states: all populated Cr states are spin-down (band *B* on the Fig. 4) and all available empty spin-down states are concentrated on the band *C*. Both bands are situated within the BGO gap, and electronic transitions between them generate the absorption peak V at the Fig. 6, centered on approximately 1.8 eV. Transitions from the band *B* to the bottom of the conduction band are spin-forbidden. Absorption structure VI, situated near the BGO absorption edge, is created by electron promotion from the band *A* at the top of the valence region to the band *C*. Since the band *A* does not contain Cr *d*-states, origin of the structure VI is attributed to the transitions from the spin-down O *p*-states to the spin-down Cr *d*-states (involving charge transfer), as well as to the transition between empty and populated O's spin-down *p*-states.

E. Comparison of calculated and experimental absorption spectrum

Figure 7 shows the calculated absorption spectra of both BGO:Cr→Ge and BGO:Cr→Bi as functions of incident radiation wavelength, compared with the experimental absorption spectrum of the Cr doped BGO recorded at ambient temperature.[10] The experimental spectrum is characterized by two broad absorption bands above the absorption threshold of the pure BGO. The first band, adjacent to the absorption edge, is situated in the wavelength range 300–600 nm with maxima at about 390, 430, and 530 nm (peaks 1, 2, and 3). The second band is centralized over the range 600–900 nm with more pronounced maxima at about 680, 740, and

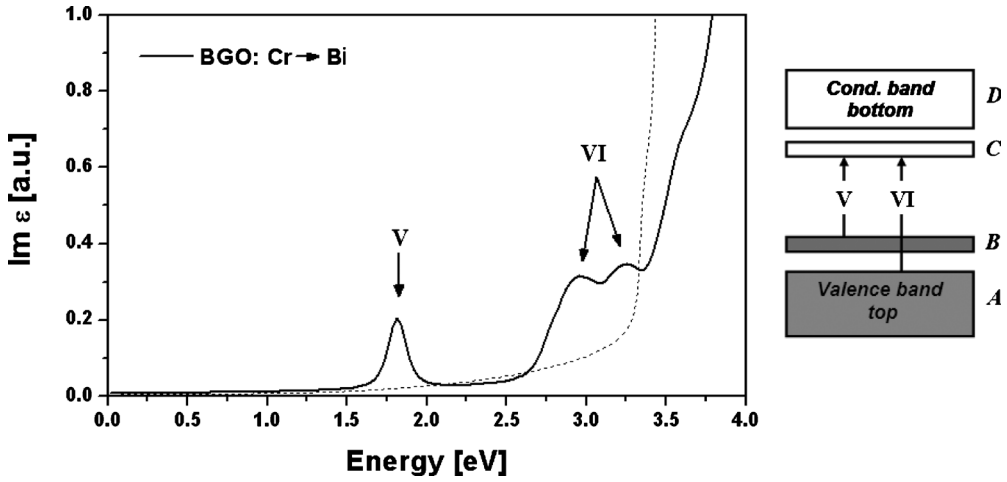

FIG. 6. Left: intensity of optical absorption of the BGO:Cr→Bi (in arbitrary units) as function of the energy of incident radiation. The dotted curve represents the optical absorption of the pure BGO. Right: energy band diagram of the BGO:Cr→Bi constructed on basis of the band structure shown at the Fig. 4, where the band notation *A*-*D* is introduced. Numbers of the vertical arrows indicate electronic transitions responsible for the corresponding structures in the optical spectrum.

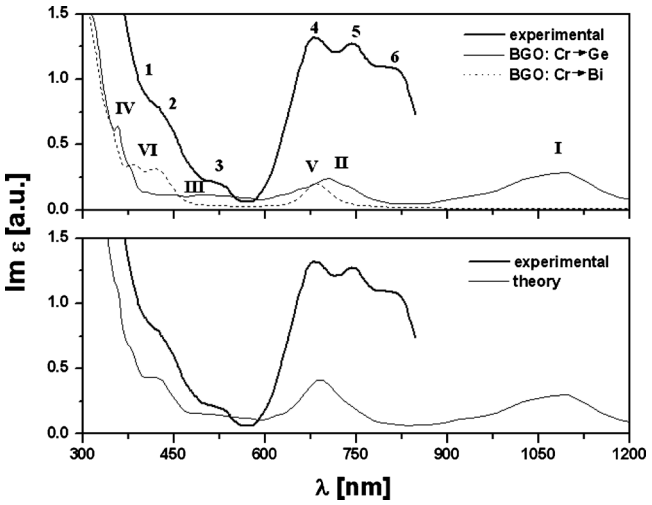

FIG. 7. Up: calculated optical absorption spectra of the BGO:Cr→Ge and BGO:Cr→Bi as functions of the wavelength of incident light, compared to the experimental spectrum of the BGO:Cr (Ref. 10); Arabic numbers denote peaks in the experimental spectrum; Roman numbers, defined at the Figs. 5 and 6 denote peaks in the calculated spectrum. Down: comparison between the BGO:Cr experimental and theoretical spectrum; the latter is obtained by superposition of the BGO:Cr→Ge and BGO:Cr→Bi spectra.

800 nm (peaks 4, 5, and 6). There has also been observed the third band, broad and spread over the range 1150–1300 nm. This band is not reported in the Ref. 10 but in the Ref. 11 in which the authors extended the measurements of absorption spectrum to infrared wavelengths.

In both experimental papers[10,11] the origin of observed spectra was discussed in terms of Tanabe–Sugano diagrams for the Cr ion accommodated at the Ge site. Both papers agree that the 600–900 nm band should be caused by transitions between the levels of the Cr^{4+} ion positioned at this site. The authors of the Ref. 10 assume that the 300–600 nm band has the same origin (involving other transitions), while the authors of the Ref. 11 suppose that this band, as well as the 1150–1300 nm one, originates from the transitions between the levels of the Cr^{3+} ion located at the Ge^{4+} site. This explanation, however, requires consideration of charge compensation, which has not been discussed in the Ref. 11.

Results of our calculations demonstrate that principal characteristics of experimental absorption spectrum can be satisfactorily interpreted by superposition of two absorption spectra produced by the Cr^{4+} and Cr^{3+} ions which substitute the Ge and the Bi ions, respectively. Such resulting theoretical spectrum, shown at the lower graph of the Fig. 7, consists of three distinct broad absorption bands, composed of the peaks I–VI defined on the Figs. 5 and 6 (Sec. III D). The three experimentally observed absorption bands can be interpreted in terms of these theoretical bands.

The infrared 1150–1300 nm band (not shown at the Fig. 7) is reproduced theoretically by somewhat broader (950–1250 nm) absorption band which clearly originates from d-d transitions of the Cr^{4+} ion (peak I). This fact shows that a complicate interpretation offered in the Ref. 11, involving Cr^{3+} ion situated at the Ge^{4+} site and requiring the charge compensation, is not necessary.

The 600–900 nm band is relatively badly reproduced by a broad band situated between 600 and 800 nm. The latter consists of just one pronounced peak, instead of experimentally registered three. The upper graph on the Fig. 7, however, shows that theoretical band has more complex structure, which is just less pronounced. The band is composed of both Cr^{4+} and Cr^{3+} contributions that involve transitions between their *d*-states (peaks II and V, respectively). This fact confronts the interpretation proposed in experimental studies[10,11] which attribute the origin of this band exclusively to the Cr^{4+}. Since, however, according to Bravo and Lopez,[9] the concentration of the Cr^{4+} is always much higher than the Cr^{3+} concentration, the 600–900 nm band should be considered as Cr^{4+} dominated.

The 300–600 nm band is pretty well reproduced theoretically by series of shoulders set against the absorption edge (structures III, IV, and VI), for which both the Cr^{4+} and Cr^{3+} are responsible. The contribution from the Cr^{4+} is, however, much less significant since intensity of the structure III is very weak and the structure IV can be considered as part of the host absorption (as discussed in the Sec. IVD). Therefore, we attribute the origin of the 300–600 nm band to the Cr^{3+} ion. This band is dominantly generated by electron transfer from the populated O *p* states to the empty *d*-states of the neighboring Cr^{3+} situated at the Bi^{3+} positions (peak VI).

Due to a fact that the calculated BGO band gap is smaller than the experimental [3.19 (Ref. 14) versus 4.96 (Ref. 23) eV], our theoretical interpretation of the BGO:Cr absorption spectrum is only qualitative. The wrong size of the gap comes from the shortcomings of the GGA to accurately describe exchange and correlation effects in DFT. Although we had a possibility to adjust the gap applying "scissors operator," we did not do it in order not to perturb the position of the Cr states relative to the valence band edge. In spite of this limitation, we think that present analysis offers enough arguments to support a conclusion that the BGO:Cr optical spectrum is composed of optical responses from both the Cr^{3+} and Cr^{4+} ions, indicating the Cr simultaneous presence at both the Bi^{3+} and Ge^{4+} sites. This conclusion is additionally enforced by defect formation energy calculations (Sec. III A) which demonstrated that the Cr is easily incorporated in either site, with no significant energy difference. The different Cr^{3+} and Cr^{4+} concentrations, observed by Bravo and Lopez,[9] result from specific chemical reactions and processes of the Cr implementation into the BGO crystal matrix, which has not been discussed in this paper.

IV. CONCLUSIONS

We have analyzed theoretically energetic, structural, electronic, and optical properties of the Cr doped BGO scintillator, taking into account the fact that Cr can substitute either Ge or Bi atom in the BGO lattice. As a computation tool it was employed the DFT based, FP-LAPW method. The results of energetic balance do not strongly indicate which site, Bi or Ge, should be preferable for substitution. The defect formation energy in the case when Cr substitutes the Ge is just 0.039 eV lower in comparison with the case when Cr substitutes the Bi. When situated at the Ge site, the Cr maintains the bond length and angles with neighboring oxy-

gens practically unchanged. When substitutes the Bi, however, the Cr significantly changes its octahedral environment, suffering large off-site departure along the C_3 axis away from the center of imaginary octahedron of O's around it. The Cr modifies electronic structure of the pure BGO introducing its *d*-states within the band gap: two deeplike occupied bands if it substitutes the Ge (Cr^{4+}) and one occupied and another unoccupied shallowlike band if it substitutes the Bi (Cr^{3+}). In the first case the Cr magnetic moment is calculated to be +1.58 μ_B while in the second −2.44 μ_B, meaning that they should be aligned oppositely in the external magnetic field. The optical absorption spectra were calculated as functions of incident light energy up to 40 eV. Absorption peaks caused by the Cr presence were identified and interpreted in terms of calculated electronic structure, for both possible Cr accommodations. Comparison with the experimental data suggests that absorption spectrum of the Cr doped BGO consists from optical responses of both Cr^{4+} and Cr^{3+} ions, indicating the Cr simultaneous presence in both Ge and Bi substitution sites.

ACKNOWLEDGMENTS

The authors gratefully acknowledge the CNPq and FAPITEC-SE (Brazilian funding agencies) for financial support.

[1]E. Auffray, F. Cavallari, M. Lebeau, P. Lecoq, M. Schneegans, and P. Sempere-Roldan, Nucl. Instrum. Methods Phys. Res. A **486**, 22 (2002).
[2]J. M. Classe, M. Fiche, C. Rousseau, C. Sagan, F. Dravet, R. Pioud, A. Lisbona, L. Ferrer, L. Campion, I. Resche, and C. Curtet, J. Nucl. Med. **46**, 395 (2005).
[3]G. Montemezzani, St. Pfandler, and P. Gunter, J. Opt. Soc. Am. B **9**, 1110 (1992).
[4]S. G. Raymond and P. D. Townsend, J. Phys.: Condens. Matter **12**, 2103 (2000).
[5]C. Zaldo and E. Moya, J. Phys.: Condens. Matter **5**, 4935 (1993).
[6]R. Y. Zhu, H. Stone, H. Newman, T. Q. Zhou, H. R. Tan, and C. F. He, Nucl. Instrum. Methods Phys. Res. A **302**, 69 (1991).
[7]A. C. S. de Mello, G. C. Santana, R. A. Jackson, Z. S. Macedo, S. G. C. Moreira, and M. E. G. Valerio, Phys. Status Solidi C **4**, 980 (2007).
[8]E. Moya, L. Contreras, and C. Zaldo, J. Opt. Soc. Am. B **5**, 1737 (1988).
[9]D. Bravo and F. J. Lopez, Opt. Mater. **13**, 141 (1999).
[10]N. V. Chernei, V. A. Nadolinnyi, N. V. Ivannikova, V. A. Gusev, I. N. Kupriyanov, V. N. Shlegel, and Y. V. Vasiliev, J. Struct. Chem. **46**, 431 (2005).
[11]Y. Huang, X. Feng, G. Hu, B. Yang, Y. Ling, W. Pang, and J. Zhu, Chin. Phys. Lett. **11**, 383 (1994).
[12]S.-Y. Wu and H.-N. Dong, Opt. Mater. **28**, 1095 (2006).
[13]M. V. Lalic and S. O. Souza, Opt. Mater. **30**, 1189 (2008).
[14]A. F. Lima, S. O. Souza, and M. V. Lalic, J. Appl. Phys. **106**, 013715 (2009).
[15]P. Hohenberg and W. Kohn, Phys. Rev. **136**, B864 (1964); W. Kohn and L. J. Sham, *ibid.* **140**, A1133 (1965).
[16]O. K. Andersen, Phys. Rev. B **12**, 3060 (1975); D. J. Singh, *Plane Waves, Pseudopotentials and the LAPW Method* (Kluwer Academic, Dodrecht, 1994).
[17]P. Blaha, K. Schwarz, G. K. H. Madsen, D. Kvasnicka, and J. Luitz, *WIEN2k, An Augmented Plane Wave + Local Orbitals Program for Calculating Crystal Properties* (Karlheinz Schwarz, Techn, Austria, 2001).
[18]J. P. Perdew, K. Burke, and M. Ernzerhof, Phys. Rev. Lett. **77**, 3865 (1996).
[19]W. D. Lynch, *Handbook of Optical Constants of Solids*, edited by E. D. Palik (Academic, New York, 1985).
[20]G. E. Jellison, Jr., S. Auluck, D. J. Singh, and L. A. Boatner, J. Appl. Phys. **107**, 013514 (2010).
[21]P. Fischer and F. Waldner, Solid State Commun. **44**, 657 (1982).
[22]S. A. S. Farias and M. V. Lalic, Solid State Commun. **150**, 1241 (2010).
[23]F. Antonangeli, N. Zema, M. Piacentini, and U. M. Grassano, Phys. Rev. B **37**, 9036 (1988).